

Metformin and AMP Kinase Activation Increase Expression of the Sterol Transporters ABCG5/8 (ATP-Binding Cassette Transporter G5/G8) With Potential Antiatherogenic Consequences

Matthew M. Molusky,* Joanne Hsieh, Samuel X. Lee, Rajasekhar Ramakrishnan, Liana Tascau, Rebecca A. Haeusler, Domenico Accili, Alan R. Tall

Objective—The mechanisms underlying the cardiovascular benefit of the anti-diabetic drug metformin are poorly understood. Recent studies have suggested metformin may upregulate macrophage reverse cholesterol transport. The final steps of reverse cholesterol transport are mediated by the sterol transporters, ABCG5 (ATP-binding cassette transporter G5) and ABCG8 (ATP-binding cassette transporter G8), which facilitate hepato-biliary transport of cholesterol. This study was undertaken to assess the possibility that metformin induces *Abcg5* and *Abcg8* expression in liver and to elucidate the underlying mechanisms.

Approach and Results—Metformin-treated mouse or human primary hepatocytes showed increased expression of *Abcg5/8* and the bile salt export pump, *Bsep*. Administration of metformin to Western-type diet-fed mice showed significant upregulation of *Abcg5/8* and *Bsep*. This resulted in increased initial clearance of ³H-cholesteryl ester HDL (high-density lipoprotein) from plasma. However, fecal ³H-cholesterol output was only marginally increased, possibly reflecting increased hepatic *Ldlr* (low-density lipoprotein receptor) expression, which would increase nonradiolabeled cholesterol uptake. *Abcg5/8* undergo strong circadian variation. Available chromatin immunoprecipitation-Seq data suggested multiple binding sites for Period 2, a transcriptional repressor, within the *Abcg5/8* locus. Addition of AMPK (5' adenosine monophosphate-activated protein kinase) agonists decreased Period 2 occupancy, suggesting derepression of *Abcg5/8*. Inhibition of ATP citrate lyase, which generates acetyl-CoA from citrate, also decreased Period 2 occupancy, with concomitant upregulation of *Abcg5/8*. This suggests a mechanistic link between feeding-induced acetyl-CoA production and decreased cholesterol excretion via Period 2, resulting in inhibition of *Abcg5/8* expression.

Conclusions—Our findings provide partial support for the concept that metformin may provide cardiovascular benefit via increased reverse cholesterol transport but also indicate increased *Ldlr* expression as a potential additional mechanism. AMPK activation or ATP citrate lyase inhibition may mediate antiatherogenic effects through increased ABCG5/8 expression.

Visual Overview—An online [visual overview](#) is available for this article. (*Arterioscler Thromb Vasc Biol.* 2018;38:1493-1503. DOI: 10.1161/ATVBAHA.118.311212.)



Key Words: ATP-binding cassette transporter ■ cholesterol ■ high-density lipoprotein ■ metformin ■ sterol cardiovascular disease

Metformin, the most widely used drug to treat diabetes mellitus, seems to offer moderate protection against atherosclerotic cardiovascular disease.^{1,2} The mechanism of this likely benefit is poorly understood. In metabolic studies, diabetics treated with metformin had a significantly lower VLDL (very low-density lipoprotein) cholesterol level in the postprandial state.³ However, metformin treatment has not been consistently associated with changes in VLDL/LDL (low-density lipoprotein) cholesterol levels in population studies.^{1,2,4} Thus, the mechanisms underlying its apparent cardiovascular benefit are unclear.⁵

Recent studies have shown that metformin increases HDL (high-density lipoprotein)-mediated reverse cholesterol transport (RCT), acting on macrophages to upregulate *Abca1/g1* which mediate the efflux of cholesterol onto and apoA-1 and HDL particles.⁶ The final step in the RCT pathway is mediated by the cholesterol half-transporters ABCG5 (ATP-binding cassette transporter G5) and ABCG8 (ATP-binding cassette transporter G8),⁷⁻⁹ which reside on the canicular membrane of hepatocytes facilitating excretion of cholesterol and plant sterols into bile. Genome-wide association studies have identified SNPs (single nucleotide polymorphisms) in the *ABCG5/8*

Received on: September 20, 2017; final version accepted on: May 16, 2018.

From the Division of Molecular Medicine, Department of Medicine (M.M.M., J.H., L.T., A.R.T.), Naomi Berrie Diabetes Center, College of Physicians and Surgeons (S.X.L., R.A.H.), Pediatrics, College of Physicians and Surgeons (R.R.), Department of Pathology and Cell Biology (R.A.H.), and Department of Medicine and Naomi Berrie Diabetes Center (D.A.), Columbia University, New York.

The online-only Data Supplement is available with this article at <http://atvb.ahajournals.org/lookup/suppl/doi:10.1161/ATVBAHA.118.311212/-/DC1>.

Correspondence to Matthew M. Molusky, PhD, Division of Molecular Medicine, Department of Medicine, Columbia University, 630 W 168th St P&S 8-401, New York, NY 10032. E-mail mmm2338@cumc.columbia.edu

© 2018 American Heart Association, Inc.

Arterioscler Thromb Vasc Biol is available at <http://atvb.ahajournals.org>

DOI: 10.1161/ATVBAHA.118.311212

Nonstandard Abbreviations and Acronyms	
ABCG5/8	ATP-binding cassette transporter G5/G8
ACLY	ATP citrate lyase
Alb-Cre	Cre recombinase driven by albumin promoter
Alb-Cre(+)Prkaa1fl/fl	hepatocyte-specific Prkaa1 knockout
AMPK	5' adenosine monophosphate-activated protein kinase
BSEP	bile salt export pump
PRKAA1	protein kinase AMP-activated catalytic subunit alpha 1
ChIP	chromatin immunoprecipitation
CHX	cycloheximide
CRY1	cryptochrome 1
DBP	D site of albumin promoter binding protein
³ H-CE	³ H cholesteryl ester
HDL	high-density lipoprotein
LDL	low-density lipoprotein
PER2	period 2
VLDL	very low-density lipoprotein
WTD	Western-type diet

locus associated with LDL cholesterol levels, total cholesterol levels, and coronary artery disease.^{10–13} *Abcg5/8* are known to be transcriptionally upregulated by the liver X receptor alpha (*LXRα*, *Nr1h3*) and by FoxO (Forkhead box O) transcription factors.^{14–17} However, other modes of regulation, including by metformin, have not been well documented. In this study, we sought to determine whether the final step of RCT mediated by ABCG5/8 might also be upregulated by metformin. This led to the discovery that Period 2 (PER2), a circadian regulator, binds and represses *Abcg5/8* mRNA expression. PER2 in turn seems to be oppositely regulated by the activities of AMPK (5' adenosine monophosphate-activated protein kinase) and ATP citrate lyase (ACLY). These findings provide a mechanism to explain how biliary cholesterol excretion is linked to hepatic lipogenic activity and the circadian cycle.

Materials and Methods

The data that support the findings of this study are available from the corresponding author on reasonable request.

Mice and In Vivo Experiments

We chose to use male mice for our studies as it has been previously reported in rodents that glucose tolerance and plasma insulin concentrations vary during the estrous cycle.¹⁸ C57BL/6J mice were purchased from Jackson Laboratory (Stock No. 000664).¹⁹ Albumin-Cre were purchased from Jackson Laboratory (Stock No. 003574)²⁰ and bred with Prkaa1 (protein kinase AMP-activated catalytic subunit alpha 1) flox/flox mice also purchased from Jackson Laboratory (Stock No. 014141)²¹ to produce mice with Prkaa1 knocked-out in liver (Alb-Cre(–) Prkaa1 fl/fl and Alb-Cre(+) Prkaa1). For chow fasting/refeeding model, C57B16/J mice were used. Mice were fasted for 14 hours, and then subsequently refeed after injection with metformin (250 mg/kg) or saline control. After 4 hours of refeeding, mice were euthanized, and liver was collected and snap frozen in liquid nitrogen. For chronic metformin treatment, C57B16/J mice were fed a western-type diet (WTD; 42% calories from fat, 0.2% cholesterol, Envigo; TD.88132) for 3 months. Subsequently mice were split into 2 groups, one group receiving 250 mg/kg metformin or saline control (IP), daily, for 2 weeks. Mice were then euthanized in the fed state and

livers were collected and snap frozen in liquid nitrogen and stored at –80°C. All protocols were approved by the Institutional Animal Care and Use Committee of Columbia University.

Primary Hepatocytes

Mouse hepatocytes were isolated using the Worthington Biochemical Corporation Hepatocyte Isolation Kit. In brief, mice were euthanized, and the livers were perfused with Hanks' Balanced Salt solution, without calcium or magnesium. After perfusion, livers were switched to digestion media (L-15/MOPS solution) containing collagenase-elastase enzyme, supplemented with DNase1. After digestion, livers were removed and placed on a 10 cm plate and minced with 1 mL further of digestion media and placed at 37°C for 5 minutes. After incubation, cells were washed in excess Leibowitz Media containing 10% FBS and spun at 300g for 3 min. Cell pellet was subsequently washed 2× with Leibowitz buffer containing 0.2% FBS and 0.5% BSA. Cells were counted and seeded at a density of 0.3×10⁶ cells per well of a six-well plate in DMEM (0.2% FBS, 0.5% BSA). Forty-five minutes after plating, cells were washed with PBS, and new media (DMEM+0.2%FBS+0.5%BSA) was added containing AMPK activators or ACLY inhibitor as described in text. Phospho-ACCl (acetyl-CoA carboxylase 1; Ser79) antibody was obtained from Cell Signaling (Clone D7D11).

RNA Isolation, cDNA, and Real-Time Quantitative Polymerase Chain Reaction

RNA was isolated using TriZol Reagent (Ambion) which was then combined with Zymogen RNA isolation kit (Quick-RNA MiniPrep). RNA was quantified using a NanoDrop 8000 Spectrophotometer (ThermoFisher). Five hundred nanogram of RNA was then used to synthesize cDNA using the Maxima First Strand cDNA Synthesis Kit (Thermo Scientific). cDNA was then diluted 10-fold for real-time quantitative polymerase chain reaction (PCR) analysis. Gene expression analysis was performed using a Step One Plus Real Time PCR system (Applied Biosciences). Fold change in gene expression was calculated using the $\Delta\Delta C_t$ method. Real-time PCR primer sequences for mouse genes are as follows: *Rplp0*, 5'-gaaactgctgcctacatccg, 3'-gctggcacagtgcctcacag; *Abcg5*, 5'-atccaacacctctatgtaaatcac, 3'-tacattattggaccagttcagtcac; *Abcg8*, 5'-cctcatcattgcttctccac, 3'-attgacctctccgagtgacatt; bile salt export pump (*Bsep*), 5'-tctgactcagtgattcttgcga, 3'-cccataaacatcagccagttgt. Human real-time PCR primer sequences are as follows: *CYCLOA*, 5'-gccatccaaccactcagct, 3'-atgttcagggtggtgacttc; *ABCG5*, 5'-tcctgaggagagtgacaagaaac, 3'-acgggaaacagattcacag; *ABCG8*, 5'-ggaaccaggaaatcctattctc, 3'-ggtcaggtcca catagaagtcag; *BSEP*, 5'-ttgctgatgtttgtgggaag, 3'-ccaaaatgagtagcagccct; *ACLY*, 5'-atcggttcaagatgctcggg, 3'-aaggcatcgtgactttgacta.

Chromatin Immunoprecipitation

Primary hepatocytes were isolated as described above, except that cells were plated on 15 cm collagen-coated plates at a density of 4.4×10⁶ cells per plate. Cells were then treated with 0.5 mmol/L metformin, 10 μmol/L A-7, or 8 μmol/L BMS (iACLY) for 10 hours. Three to 4 animals were used for each chromatin immunoprecipitation (ChIP) and pooled for pull down. For RNA Pol II (Santa Cruz Biotechnology; H-224) and H3K4me3 (Abcam; ab8580) pull down, hepatocytes were washed 2 times with PBS and then cross-linked in 1% formaldehyde (Thermo Scientific, methanol-free; in PBS) for 15 min at room temperature. Cross-linking reaction was quenched with addition of 0.125 mol/L glycine and incubated for 10 min at room temperature. Quenching reaction was performed a subsequent time with fresh 0.125 mol/L glycine (in PBS) for another 10 min. Cells were then washed 3× with cold PBS and scrapped off plate in PBS and spun at 4000 rpm for 8 min. Supernatant was aspirated, and cells were resuspended in 3 mL of Nuclei Isolation Buffer (10 mmol/L Hepes [pH 7.4], 10 mmol/L KCl, 0.3% IGEPAL, Halt Protease and Phosphatase inhibitors [Thermo Scientific], 1 mmol/L PMSF, 1 mmol/L DTT, and 0.15 mmol/L spermine) and incubated on ice for 10 min. Samples were then transferred to a 10 mL dounce homogenizer and dounced 20 to 25 times to isolated nuclei. Crude

nuclei were spun at 1500 rpm for 8 min and resuspended in 200 μ L of micrococcal nuclease reaction buffer (20 mmol/L Tris-HCl [pH 8.0], 1% Triton-X100, 0.1% IGEPAL, 137 mmol/L NaCl). For PER2 (Alpha Diagnostic International, PER21-A) and cryptochrome 1 (CRY1; Alpha Diagnostic International, CRY11-A) pull down, cells were initially cross-linked with Di-(N-succinimidyl) glutarate (DSG, CovaChem; PBS, 12% DMSO) for 30 min at room temperature. Hepatocytes were washed with PBS and cross-linked with 1% formaldehyde for 15 min at room temperature and quenched and processed as described earlier.

Crude nuclei were then digested with micrococcal nuclease (New England Biolabs, M0247S) at 37°C to produce DNA fragments between 1 and 4 histone lengths (\approx 100–500 bp). Reactions were stopped by addition of excess EDTA (10 mmol/L final concentration). Samples were sonicated twice using a Fisher Scientific Sonic Dismembrator (Model FB120) at 40% amplitude for 15 s (30 s rest). Lysates were spun at 13 200 rpm for 2 min to remove insoluble fraction. Protein quantification of lysate was performed using a BCA Protein Assay Kit (Pierce). Forty microgram of protein was used for RNA Pol II and H3K4me3 pull down, while PER2 and CRY1 pull down was performed with 400 μ g of protein.

IP reactions were diluted to 1 mL in MNase buffer (1 mmol/L PMSF, 1 mmol/L EDTA, Halt Protease and Phosphatase inhibitors). Lysates were cleared with Protein G Dynabeads (Invitrogen) for 1 hour at 4°C, after which time Dynabeads were removed (2.5% was removed for input), and 1 μ g of anti-H3K4me3, 1 μ g anti-RNA Pol II, 5 μ g anti-PER2, or 5 μ g anti-CRY1 were added to corresponding tubes along with IgG to control tubes. Immunoprecipitations were allowed to rotate overnight at 4°C. After overnight incubation, 30 μ L of Protein G Dynabeads were added to each tube and allowed to incubate for another 2 hours. Dynabeads were separated using a DyanMag-2 (Invitrogen) magnet. Dynabeads were washed 2 \times with MNase Buffer, Wash Buffer 2 (20 mmol/L Tris-HCl [pH 8.0], 1% Triton-X100, 0.1% SDS, 500 mmol/L NaCl, 2 mmol/L EDTA), Wash Buffer 3 (20 mmol/L Tris-HCl [pH 8.0], 1% Triton-X100, 250 mmol/L LiCl, 2 mmol/L EDTA), and 1 \times with TE buffer (10 mmol/L Tris-HCl, 1 mmol/L EDTA).

To elute bound DNA, Dyanbeads were resuspended in 100 μ L of SDS elution buffer (50 mmol/L NaHCO₃, 1% SDS) and agitated for 15 min at room temperature. Supernatant was separated from beads using a magnet and placed in a new tube. A second elution was performed with 100 μ L of elution buffer and incubated at 55°C for 15 min. Supernatant was again separated from beads using a magnet and was added to previous elution. NaCl was added to each sample to a final concentration of 250 mmol/L and incubated at 65°C overnight to reverse cross-link. Samples were then treated with RNaseA (10 μ g/sample, 1 hour, 37°C) and then digested with Proteinase K (80 μ g/sample, 55°C, 2 hours). DNA was isolated using QiaQuick columns (Qiagen) and eluted in ddH₂O. Isolated DNA was stored at –80°C. Recovered DNA was quantified using Step One Plus Real Time PCR system (Applied Biosciences). Percent occupancy was calculated relative to input for each sample. ChIP primer sequences are as follows: *Abcg5/8* promoter, 5'-gagcgttgacctgtgaact, 3'-tatggcaagcgtagc-gatct; *Bsep* promoter, 5'-gcactgctgtaagaccgttacc, 3'-gcttggttagcgtg-gaac; *Dbp* (D site of albumin promoter binding protein) enhancer, 5'-acaccgcatccgatgac, 3'-ccacttcggccaatgag.

HDL ³H-Cholesteryl Ester Kinetics Studies

³H-Cholesteryl ester (³H-CE) HDL kinetics studies were performed as previously described.^{22–24} Briefly, 1mCi ³H-cholesterol was added to a 1:1 mixture of HDL and LCAT (lecithin cholesterol acyltransferase) and incubated for 3 hours at 37°C. ³H-HDL was recovered using ultracentrifugation, where it was added back to LDL (repeated twice) and incubated for 3 hours at 37°C. HDL was isolated once again using ultracentrifugation where it was then dialyzed against KBr overnight and subsequently sterile filtered through a 0.22 μ m filter and stored at 4°C until injection. Mice were injected intravenously, and blood was taken at 0, 2, 4, 8, and 24 hours postinjection. Feces were collected over the course of 2 days. Feces were dried overnight in a 60°C oven, and the ³H-cholesterol was isolated using the Folch lipid extraction method.²⁵

Plasmid and siRNA Transfections

HEK293 cells were transfected overnight with 500 ng of Flag-mPer2 plasmid and 10 ng of either siAcly (Dharmacon SMART Pool) or siRNA control using Lipofectamine 2000 in OptiMem media, which was replaced next day with DMEM+10% FBS. Forty-eight hours later, media was aspirated and replaced with DMEM+10% FBS containing 50 μ g/mL cycloheximide. At indicated time points, cells were washed with PBS harvested in 250 μ L of RIPA buffer (Halt Protease and Phosphatase inhibitors, 1 mmol/L PMSF, and 1 mmol/L EDTA). Cell lysates were sonicated 3 times at 50% amplitude for 15 s. Lysates were spun at 13 200 rpm for 3 min to remove precipitate. Protein was quantified using Pierce BCA Protein Assay Kit and run on an SDS-PAGE gel. For Flag-mPer2,²⁶ Flag-mCry1,²⁶ and Acly (S455D)^{27,28} cotransfections, HEK293 cells were transfected as described earlier, but 250 ng of each plasmid was used (250 ng Per2+250 ng Acly (S455D); 250 ng Cry1+Acly S455D). Where Acly (S455D) was not transfected, pCAG-RFP plasmid was used to make the total plasmid DNA transfected 500 ng per well. Anti-mouse anti-Flag (Sigma) was used to detect PER2 and CRY1. Flag-mPer2 (pP2BA) was a gift from Aziz Sancar (Addgene plasmid No. 31369). Flag-mCry1 (pMC1SG5) was a gift from Aziz Sancar (Addgene plasmid No 31282). Acly (S455D) was a gift from Kathryn Wellen (Addgene plasmid No 70768).

Statistical Analysis

All values are reported as mean \pm SD or SEM where indicated. Data were analyzed using Student *t* tests, unpaired *t* test with Welch's correction, one-way analysis of variance, or 2-way analysis of variance with Tukey's post hoc test where indicated. Tests were validated for normalcy using either D'Agostino & Pearson or Shapiro-Wilk normality tests, and variance was tested using the *F* test or Brown-Forsythe (analysis of variance). Statistical analysis was performed using Prism 7 (GraphPad) software.

Results

Metformin Induces *Abcg5* and *Abcg8* in Primary Hepatocytes and Liver

We treated mouse primary hepatocytes with 0.5 mmol/L metformin for 20 hours and found a marked upregulation of both *Abcg5* and *Abcg8* mRNAs along with the bile salt transporter, *Bsep* (*Abcb11*) (Figure 1A). Because metformin indirectly activates AMPK through interactions with mitochondrial proteins,²⁹ we sought to establish whether the upregulation of *Abcg5/8* was because of direct activation of AMPK. To this end, we used the AMPK-specific agonist A-769662³⁰ in primary hepatocytes and found that in a dose-dependent manner A-769662 was able to induce *Abcg5* and *Abcg8* mRNA (Figure 1B). We observed similar effects on expression of *ABCG5*, *ABCG8*, and *BSEP* in primary human hepatocytes treated with AICAR (5-aminoimidazole-4-carboxamide ribonucleotide; Figure 1C), suggesting a conserved pathway between mice and humans. The relative levels of *Abcg5* and *Abcg8* mRNA decrease rapidly after initial plating (data not shown); however, Ct values were still in the range of 29 to 32 for *Abcg5* and *Abcg8* in our primary hepatocyte culture experiments (Table I in the [online-only Data Supplement](#)).

Previous work has established the hormonal regulation of AMPK activity during fasting and feeding.^{31–34} Consistent with the cell culture results, we observed an increase in *Abcg5/8* mRNA in fasting versus refeed livers (Figure 1D). We also used a fasted/refed rodent model to test metformin induction of *Abcg5/8* in vivo. After a bolus of metformin, there was a modest but significant upregulation of *Abcg5* and *Abcg8* in the refeed group (n=15) compared with a saline control

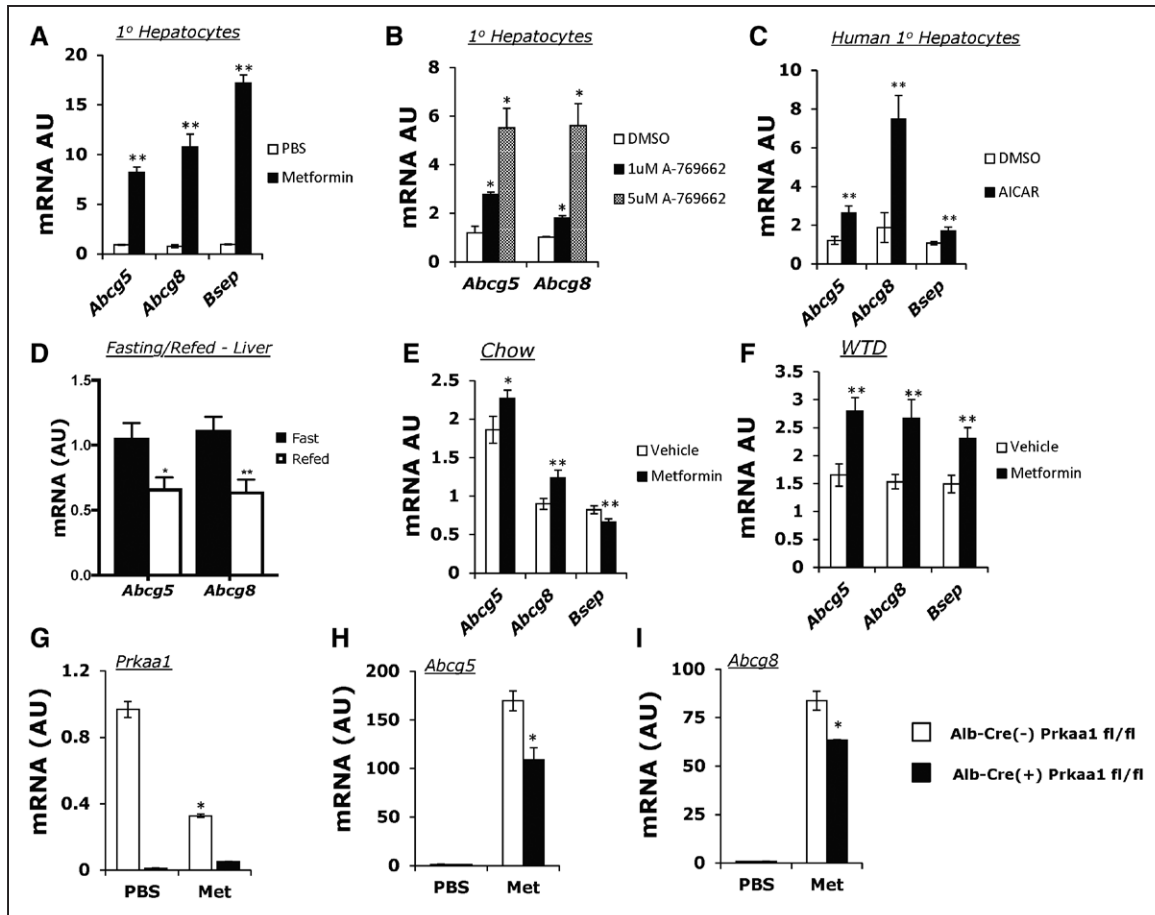


Figure 1. AMPK (5' adenosine monophosphate-activated protein kinase) activation results in the upregulation of the liver cholesterol efflux genes, *Abcg5/Abcg8* (ATP-binding cassette transporter G5/G8) in hepatocytes and liver. **A**, Real-time polymerase chain reaction (PCR) gene expression analysis of mouse primary hepatocytes treated with 0.5 mmol/L metformin for 20 hours in DMEM (0.2% FBS). **B**, Real-time PCR gene expression analysis of mouse primary hepatocytes treated with 2 doses, 1 and 5 μ mol/L of A-7, an AMPK-specific agonist for 20 hours. **C**, Human primary hepatocytes treated with AICAR (5-aminoimidazole-4-carboxamide ribonucleotide; black bar; 0.5 μ mol/L, 6 hours) or DMSO control (white bar). **D**, *Abcg5* and *Abcg8* expression in fasting (black bar) or refed (white bar) livers (n=4–5). **E**, Gene expression analysis of a fasting/refeeding protocol with a single 250 mg/kg metformin bolus during refeeding (n=15). **F**, Real-time PCR gene expression of the livers of mice fed a Western-type diet (WTD) for 3 months with a 2-week regimen of metformin (n=7; 250 mg/kg). **F–H**, Real-time quantitative PCR analysis of metformin treatment (0.5 μ mol/L, 20 hours) in Alb-Cre(-)Prkaa1 fl/fl (white bar) and Alb-Cre(+) Prkaa1 fl/fl (black bar) primary hepatocytes looking at *Prkaa1* (**G**), *Abcg5* (**H**), and *Abcg8* (**I**) expression. **A**, **C**, **E**, **F**, Data represents mean \pm SEM; **P*<0.05, ***P*<0.01 using multiple *t* tests (FDR<0.05). **B** and **D**, Data represents n=3 \pm SD; **P*<0.05, ***P*<0.01 using unpaired Student *t* test. **G–I**, Data represents mean \pm SD; **P*<0.05 using 2-way analysis of variance (ANOVA) with Tukey's multiple comparisons test.

refed group (Figure 1E). AMPK activity has been shown to be downregulated in high-fat diet-fed mice,^{35,36} and therefore we sought to determine whether increasing AMPK signaling would upregulate *Abcg5* and *Abcg8* more prominently after feeding such a diet. We fed C57BL/6J mice a WTD (42% fat/cal, 0.2% Chol) for 3 months, then placed mice on metformin (250 mg/kg/d, IP) or saline intraperitoneally for 2 weeks and then euthanized them in the fed state. Consistent with our primary hepatocyte data, metformin prominently induced the expression of *Abcg5*, *Abcg8*, and *Bsep* compared with the saline control (Figure 1F; *P*<0.05).

Mice carry 2 isoforms of the catalytic subunit of AMPK, α 1, α 2 (*Prkaa1*, *Prkaa2*), which are thought to be similarly expressed in liver; however, *Prkaa1* has been shown to rhythmically localize to the nucleus which may aid in regulating transcriptional activity.³⁷ To examine the AMPK dependence of metformin-induced expression of *Abcg5/8*, we bred Albumin-Cre (Alb-Cre) with *Prkaa1* floxed mice (fl/fl). In

the *Prkaa1* knockout (Alb-Cre(+) *Prkaa1* fl/fl) hepatocytes, there was a significant reduction in *Abcg5/8* mRNAs after metformin treatment compared with floxed controls (Alb-Cre(-) *Prkaa1* fl/fl) (Figure 1G through 1-I; **P*<0.05). This indicates that regulation of *Abcg5/8* by metformin depends at least in part on intact AMPK signaling. The residual increase in *Abcg5/8* expression in Alb-Cre(+) *Prkaa1* fl/fl mice could reflect activity of *Prkaa2* or an independent pathway, which has recently been demonstrated, where an AMPK β -specific subunit agonist induction of *Abcg5/8* was in abolished α 1/ α 2 knockout livers.³⁸

Induction of *Abcg5/8* Expression Does Not Require LXR or FoxO Transcription Factors

LXR α , the predominant isoform of LXR expressed in the liver,^{39–41} has been shown to mediate induction of *Abcg5* and *Abcg8* in response to feeding a high cholesterol diet.¹⁴ However, in primary hepatocytes lacking LXR α , the main

isoform of LXR expressed in the liver, there was no difference in the induction of *Abcg5/8* compared with wild-type controls (Figure I in the [online-only Data Supplement](#)). In addition, the FoxO family of transcription factors has been shown to induce *Abcg5/8*, providing a link between hepatic insulin resistance and gallstone formation.¹⁶ However, the induction of *Abcg5/8* was actually more pronounced in response to AMPK activators in FoxO triple knockout (FoxO1/3/4, FoxO TKO) hepatocytes (Figure IIA and IIB in the [online-only Data Supplement](#)), indicating involvement of an alternative regulatory pathway. FoxO TKO hepatocytes did show reduced induction of *Bsep* when treated with AICAR compared with wild-type controls (Figure IIC in the [online-only Data Supplement](#)), consistent with previous reports.¹⁷

AMPK Activation Increases *Abcg5/8* Transcriptional Activity

To determine if AMPK activators require new transcription to induce *Abcg5/8* expression in primary hepatocytes, we treated cells with the transcription inhibitor actinomycin D⁴² in the presence or absence of AICAR. Interestingly, we found that actinomycin D alone was able to induce *Abcg5/8* mRNA and that addition of AICAR had no further additive effect (Figure 2A). Moreover, inhibiting protein synthesis using CHX (cycloheximide) resulted in increased expression of *Abcg5/8*, as well as *Bsep*, and again there was no additional effect of AICAR in the presence of CHX (Figure 2B). These observations suggested that *Abcg5/8* gene expression might be repressed by a short-lived transcriptional inhibitor. Furthermore, we saw an increase in RNA Polymerase II binding at the *Abcg5/8* promoter, indicating enhanced transcription (Figure 2C), and a significant elevation in H3K4me3 at the promoters of *Abcg5/8* and *Bsep*, an epigenetic mark suggesting more transcriptionally active chromatin at the *Abcg5/8* locus (Figure 2D). Together these results indicate that AMPK activation increases transcription at the *Abcg5/8* and *Bsep* loci, possibly via inhibition of the activity of a short-lived transcriptional repressor.

Binding of PER2 to the *Abcg5/8* Locus Is Decreased by AMPK Activation

Many hepatic genes involved in metabolic processes are regulated in a circadian pattern.⁴⁵ Mining microarray datasets,⁴³ we observed a strong rhythmicity of *Abcg5/8* with suppression of expression during the dark phase (Figure 2E), suggesting that the core circadian clock machinery could play a transcriptional regulatory role. Another core clock gene ChIP-seq database⁴⁴ showed increased binding of Period 2, a repressor of transcription,^{46,47} over the *Abcg8* promoter, paralleling the suppression of *Abcg8* mRNA expression and Pol II binding during the dark phase with opposite findings during the light phase (Figure 2F).

AMPK signaling is known to decrease the stability of Period 2 indirectly through the action of a second kinase, CK1 ϵ (casein kinase 1-epsilon) and also directly via phosphorylation of PER2 heterodimer partner, CRY1.^{37,48} PER2 protein levels are also rapidly decreased by CHX treatment, consistent with our data suggesting a short-lived transcriptional repressor

(Figure 2B). We used a well characterized PER2 antibody^{49,50} to perform ChIP on primary hepatocytes treated with vehicle, metformin or A-769662. Using primers designed within the bicistronic promoter shared by *Abcg5* and *Abcg8*, we found a significant decrease ($P < 0.01$) in PER2 binding in the presence of metformin or A-769662 compared with vehicle control (Figure 3A). To validate the ChIP antibody for PER2, we used published ChIP primers⁴⁴ against a known PER2 target, *Dbp*, showing the expected decrease ($P < 0.001$) in PER2 binding within the *Dbp* upstream enhancer (Figure 3B). Additionally, CRY1 occupancy within the *Abcg5/8* promoter was decreased ($P < 0.01$) on activation of AMPK (Figure 3C).

Metformin Increases Clearance of ³H-CE in Mice on a Western-Type Diet

Given the role of *Abcg5/8* in reverse cholesterol transport, we next sought to test whether metformin treatment increased cholesterol secretion to feces. We placed mice on a Western-type diet and injected them with metformin (250 mg/kg/d, IP) for 2 weeks at the end of which we injected with HDL containing ³H-CE (intravenously). Three days before HDL injection, mice were given Ezetimibe (oral gavage, daily) to block cholesterol uptake via NPC1L1 in enterocytes. After injection, we took blood at 2, 4, 8, and 24 hours. Feces were also collected over a 2-day period of time, at which point mice were euthanized. Metformin-treated mice showed an increased rate of cholesterol clearance at 2 hours postinjection (Figure 4A; $*P < 0.05$, two-way analysis of variance) compared with vehicle-treated mice. Using a 2-pool nonlinear model, we saw a significant increase in the initial clearance rate of ³H-CE (Figure 4B) in metformin-treated mice. We saw no difference in hepatic ³H-CE uptake (Figure IIIA in the [online-only Data Supplement](#)), while the fractional catabolic rate was similar between both groups (Figure IIIB in the [online-only Data Supplement](#)). The fractional flux to the side pool was also significantly increased in metformin-treated mice, while the turnover constant of the side pool remained similar between both groups (Figure IIIC and IIID in the [online-only Data Supplement](#)). However, while elevated, the excretion of ³H-cholesterol in feces was not significantly increased in metformin-treated mice (Figure 4C; $P = 0.20$). One possible explanation for the latter finding could be an increase in uptake of LDL cholesterol in the liver of metformin-treated mice, decreasing the specific activity of hepatic ³H-cholesterol. There was a significant increase in *Ldlr* (low-density lipoprotein receptor) mRNA levels in WTD-fed mice treated with metformin (Figure IIIE in the [online-only Data Supplement](#); $*P < 0.05$). Another possibility is that metformin is increasing *Abcg5/8* mRNA. However, there was no change in enterocyte *Abcg5* or *Abcg8* mRNA in metformin-treated mice (Figure IIIG in the [online-only Data Supplement](#)).

Inhibition of ACLY Induces *Abcg5/8* Expression in Primary Hepatocytes

Given that PER2 is a transcriptional inhibitor of *Abcg5/8* expression, and is opposed by AMPK activation, we sought additional evidence for a role of this pathway in the regulation of *Abcg5/8* expression. PER2 is stabilized by the acetyl-CoA-driven acetylation of lysine residues, which inhibits

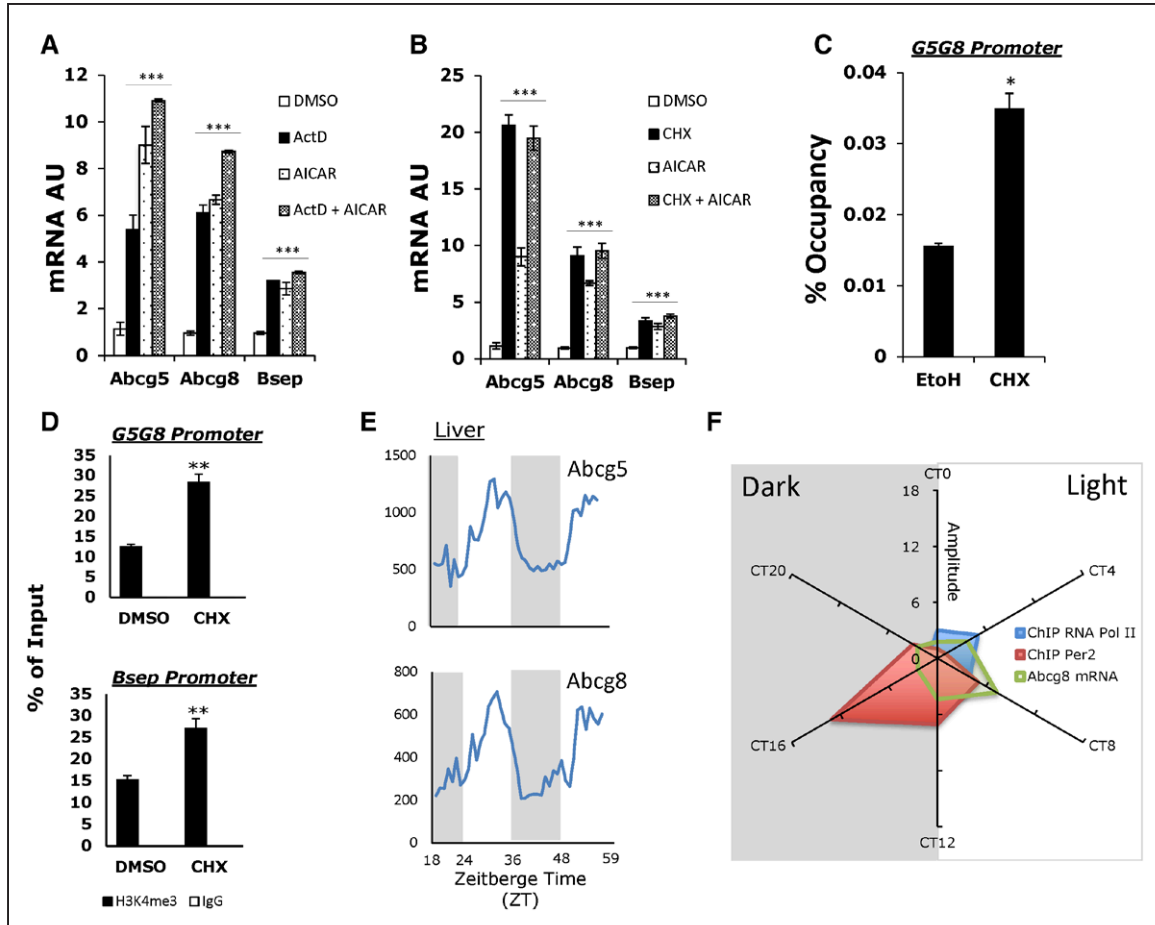


Figure 2. AMPK (5' adenosine monophosphate-activated protein kinase) activation increases *Abcg5/8* (ATP-binding cassette transporter G5/G8) transcriptional activity. **A**, Real-time quantitative polymerase chain reaction (PCR) analysis of *Abcg5*, *Abcg8*, and *Bsep* expression in primary hepatocytes treated with actinomycin (ActD), with or without AICAR (5-aminoimidazole-4-carboxamide ribonucleotide) for 6 hours. **B**, Real-time qPCR analysis of *Abcg5*, *Abcg8*, and *Bsep* expression in primary hepatocytes treated with CHX (cycloheximide) with or without AICAR for 6 hours. **C**, RNA Pol II chromatin immunoprecipitation assay (ChIP) using primers against the *Abcg5/8* bi-cistronic promoter. **D**, ChIP assay using either H3K4me3 antibody or IgG control in primary hepatocytes treated with CHX. Primers designed against the *Abcg5/8* promoter and *Bsep* promoter. **E**, Liver microarray data of *Abcg5* and *Abcg8* expression over 2 days from Hughes et al.⁴⁴ **F**, Radial plot of relative amplitude of RNA Pol II binding (blue), PER2 binding to *Abcg5/8* promoter, and *Abcg8* mRNA (green) as described in Koike et al.⁴⁴ **A** and **B**, Data represents mean±SD; ****P*<0.001 using 1-way analysis of variance (ANOVA) with Tukey's post hoc test. **C** and **D**, Data represents mean±SD; **P*<0.05, ***P*<0.01 using Student *t* test.

ubiquitin-driven proteasomal degradation.⁵¹ Acetyl-CoA can be generated from mitochondrial-derived citrate by ACLY.^{52,53} It has been established in mice that PER2 protein is increased during the night phase of the circadian cycle^{51,54} corresponding

to increased nutrient intake and increased acetyl-CoA generation. We therefore postulated that acetyl-CoA produced by ACLY could affect PER2 acetylation, as well as stability, and therefore modulate the expression of *Abcg5/8*. We used

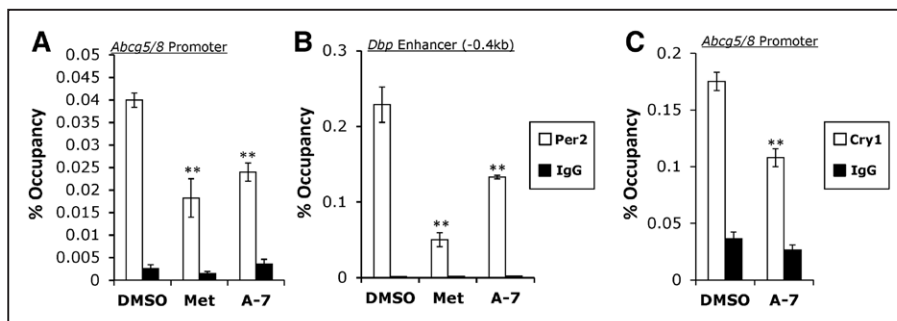


Figure 3. Period 2 (PER2) and cryptochrome 1 (CRY1) have decreased binding at the *Abcg5/8* (ATP-binding cassette transporter G5/G8) promoter when treated with AMPK (5' adenosine monophosphate-activated protein kinase) activating compounds, metformin, or A-769662. Chromatin immunoprecipitation (ChIP) assay pulling down endogenous Per2 (**A** and **B**) or Cry1 (**C**) at the *Abcg5/8* promoter (**A** and **C**) or at the proximal *Dbp* promoter (**B**), a known PER2 binding locus. Data represents mean±SD; **P*<0.05, ***P*<0.01 using Student *t* test.

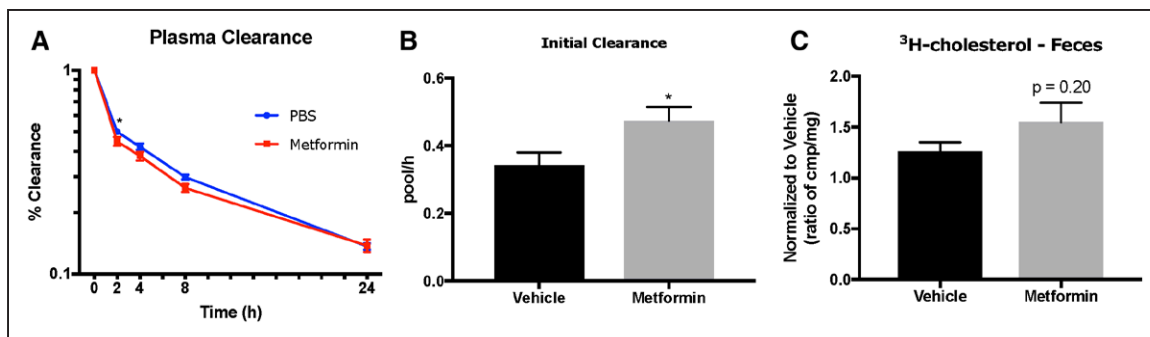


Figure 4. Metformin increases ³H-cholesterol clearance in plasma with trend of increased ³H-cholesterol in feces. **A**, Log-scale plot of percent clearance (% clearance) of ³H-cholesterol in vehicle (blue line) or metformin (red line) treated mice. **B**, Initial clearance of ³H-cholesterol using a 2-pool nonlinear modeling of individual plasma clearance curves. **C**, Measurement of ³H-cholesterol in feces of vehicle treated (black bar) or metformin treated (gray bar). Data are represented as mean±SEM of vehicle (n=10) or metformin (n=11). *P<0.05 using 2-way analysis of variance (ANOVA; **A**) or unpaired Student *t* test (**B**) or unpaired *t* test with Welch's correction (**C**).

the ACLY inhibitor BMS 303141 (referred to in figures as iACLY)^{55,56} to treat primary hepatocytes over a time course similar to that of metformin treatment. This resulted in a significant upregulation of *Abcg5*, *Abcg8*, and *Bsep* in our primary hepatocyte model (Figure 5A), paralleled by a decreased occupancy of PER2 at the *Abcg5/8* promoter (Figure 5B). There was also a significant decrease in PER2 binding at the *Dbp* locus (Figure 5C), consistent with a modification of PER2 rather than a locus-specific effect. The regulation of *Abcg5/8* by inhibition of ACLY does not require intact AMPK signaling, as *Prkaa1* KO hepatocytes responded similarly to wild-type hepatocytes (Figure 5D). Additionally, inhibition of

ACLY did not result in increased ACC1 (Ser79) phosphorylation, a known target of AMPK, compared with metformin treatment (Figure 5E). This suggests that ACLY is not acting upstream of AMPK to regulate *Abcg5/8* expression, but rather is acting through a parallel pathway or downstream of AMPK activity.

ACLY Activity Regulates Stability of PER2

Because we observed decreased PER2 binding at the *Abcg5/8* locus with ACLY inhibition, we sought additional evidence that ACLY regulates PER2 stability. Thus, we knocked down *Acly* expression by siRNA (Figure 6A) in HEK293A cells

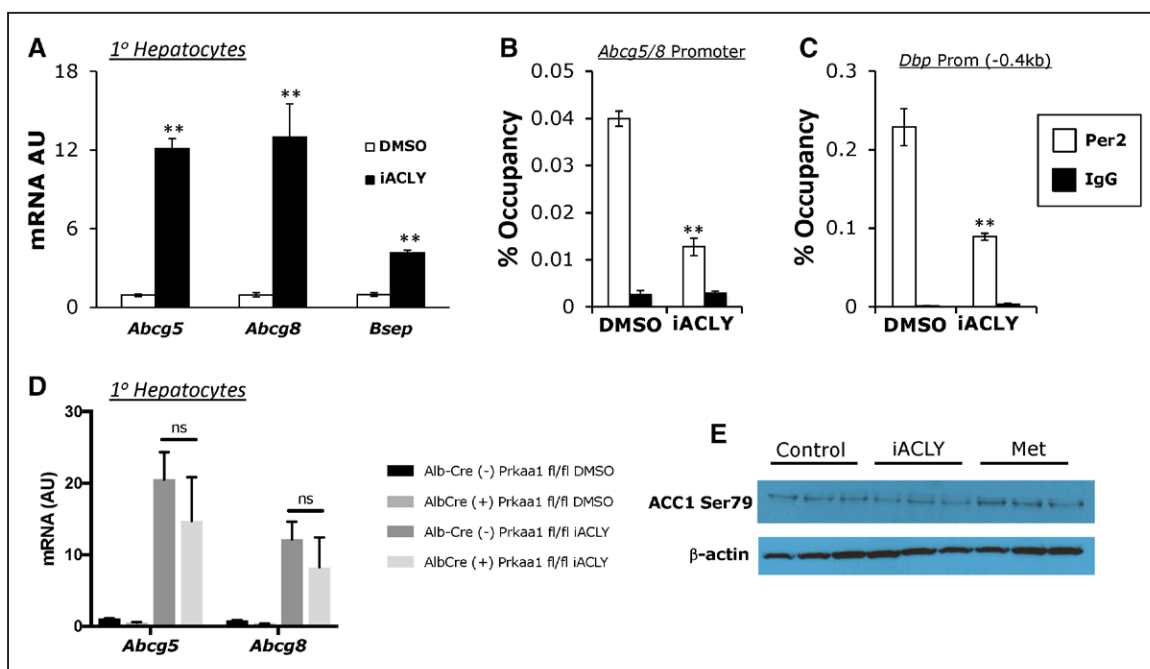


Figure 5. Inhibition of ATP citrate lyase (ACLY) results in the increase in *Abcg5/8* (ATP-binding cassette transporter G5/G8) expression accompanying a reduction of period 2 (PER2) at *Abcg5/8* promoter in primary hepatocytes. **A**, Real-time quantitative polymerase chain reaction (qPCR) analysis of *Abcg5*, *Abcg8*, and *Bsep* in primary hepatocytes treated with ACLY inhibitor, BMS 303141 (8 μmol/L), for 20 hours (n=3). **B**, Chromatin immunoprecipitation (ChIP) assay using endogenous Per2 antibody at the *Abcg5/8* promoter or (**C**) *Dbp* promoter in primary hepatocytes treated with DMSO or iACLY (n=3–4 pooled). **D**, Real-time qPCR analysis of *Abcg5* and *Abcg8* in primary hepatocytes from *Prkaa1* wild-type (WT) and *Prkaa1* knockout (KO) animals treated with ACLY inhibitor, BMS 303141 (8 μmol/L) for 20 hours (n=3). **E**, Western blot of phosphorylation of ACC1 (acetyl-CoA carboxylase 1) at Ser 79 in cells treated with iACLY (8 μmol/L) or metformin (0.5 mmol/L) for 20 hours. Data represents mean±SD. *P<0.05, **P<0.01 using unpaired Student *t* test. **B** and **C**, Data represents mean±SD using ordinary 2-way analysis of variance (ANOVA) with Tukey's multiple comparisons test (**D**).

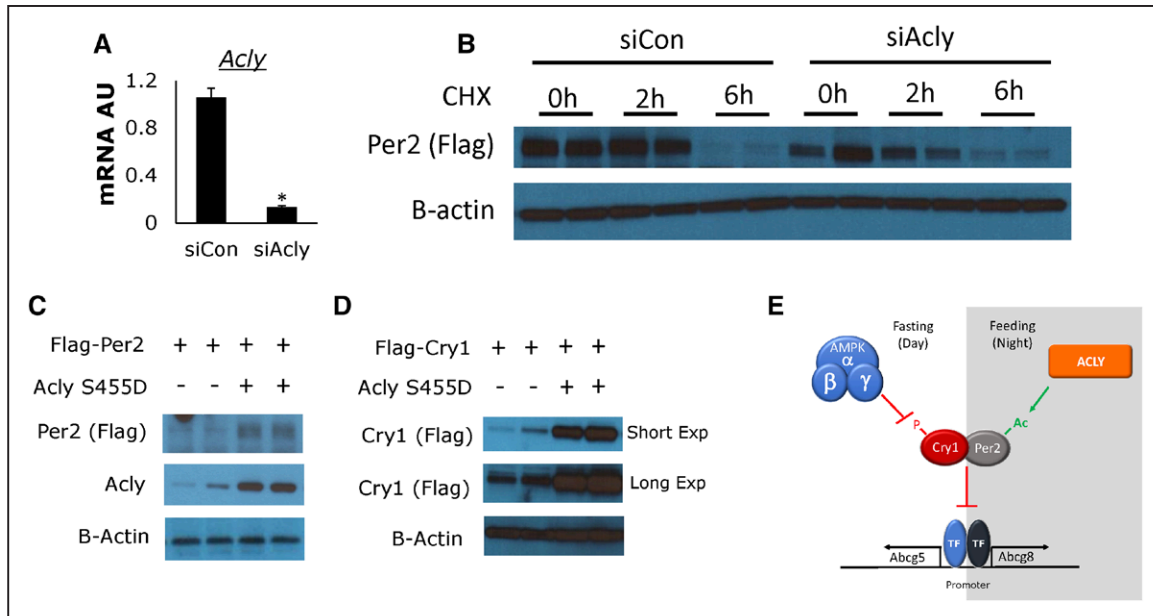


Figure 6. ATP citrate lyase (ACLY) activity regulates stability of Period 2 (PER2). **A**, Real-time quantitative polymerase chain reaction (qPCR) analysis of *Acly* expression in HEK293A cells transfected with siRNA against *Acly* or control, nonspecific siRNA. **B**, HEK293A cells cotransfected with Flag-tagged mPER2 with control siRNA or *Acly* siRNA, which were then treated with 50 μ M CHX (cycloheximide) for 0, 2, or 6 hours. **C** and **D**, HEK293A cells cotransfected with Flag-tagged mPER2 (**C**) or Flag-tagged mCRY1 (**D**), with or without a constitutively active form of ACLY, ACLY (S455D). **E**, Schematic representation of opposite effects of AMPK (5' adenosine monophosphate-activated protein kinase) and ACLY on PER2/CRY1 repressive effects on *Abcg5/8* (ATP-binding cassette transporter G5/G8) mRNA. Data represents mean \pm SD; * P <0.05, using unpaired Student t test.

expressing Flag-tagged PER2²⁶ and then treated cells with CHX (50 μ M). There was lower expression of PER2 protein at the 2-hour time point, suggesting that by limiting *Acly* we increased the turnover of PER2 (Figure 6B). Conversely, when we overexpressed a constitutively active form of ACLY, ACLY(S455D),^{27,28} we observed an increase in the overall levels of PER2, suggesting that increased production of acetyl-CoA increased PER2 stability (Figure 6C). Similarly, when we overexpressed ACLY(S455D) and Flag-tagged CRY1,²⁶ we observed increased protein expression of CRY1 (Figure 6D). As CRY1 has not been shown to be acetylated, the increased protein levels of CRY1 could be because of increased endogenous PER2, which has been shown to block CRY1 interactions, the E3 ubiquitin ligases and subsequent proteasomal degradation.^{57–60}

Discussion

Our studies in mice and in primary mouse and human hepatocytes indicate that metformin and AMPK activation induce expression of *Abcg5* and *Abcg8*, complementing recent studies from the Steinberg laboratory showing that metformin increases macrophage RCT in mice by upregulating *Abcal/g1* expression in macrophages.⁶ Given the strong link between *ABCG5/8* expression and coronary artery disease in humans,^{11–13} this suggests a novel mechanism to explain the apparent benefit of metformin treatment in cardiovascular disease. AMPK activation was shown to decrease the binding of a circadian transcriptional repressor, PER2, at the *Abcg5/8* promoter, providing a mechanism to explain increased *Abcg5/8* expression (and biliary cholesterol excretion) during fasting/daytime in mice. These observations are consistent with rodent models of circadian cholesterol efflux to

bile. In rats, maximum cholesterol secretion into bile occurs at or near the day to night transition, while maximum bile salt output occurs in the dark phase, slightly lagging behind cholesterol secretion.⁶¹ In humans with the opposite circadian rhythm, bile becomes supersaturated with cholesterol (lithogenic) during fasting at night, and cholesterol crystals become prominent in bile with diets involving prolonged fasting.^{62–65} Interestingly, similar increases in *Abcg5/8* expression in association with decreased PER2 binding to the *Abcg5/8* promoter were observed in response to ACLY inhibition. Our studies suggest that increased ACLY activity (eg, during feeding) results in increased acetylation of PER2, thereby decreasing the expression of *Abcg5/8*, while AMPK activation (during fasting and the light phase) promotes the degradation of CRY1 and PER2 and increases *Abcg5/8* expression (Figure 6E).

These findings may provide an AMPK-coordinated mechanism underpinning the balance of cholesterol disposition in hepatocytes between esterification/secretion in VLDL versus excretion into bile. AMPK acts to decrease fatty acid biosynthesis and to increase fatty acid oxidation,^{32,66} decreasing cholesterol esterification. The upregulation of *Abcg5/8* in fasting liver resulting from AMPK activation may then facilitate removal of excess cholesterol (ie, not being incorporated into VLDL particles or esterified with fatty acids into cholesteryl esters) by excretion into bile. Similarly, inhibiting ACLY and therefore reducing de novo lipogenesis could result in an increase in *Abcg5/8*, which provides a mechanism to dispose of cholesterol by excretion. Additional transcriptional control of *Abcg5/8* expression is known to be exerted via LXR and FOXO transcription factors. While the effects of AMPK activation were independent of LXR and FOXO1/3/4 in cultured

hepatocytes, the more pronounced effect of metformin on *Abcg5/8* expression in mice fed the WTD could be related to an effect of LXRs to open chromatin at the locus, increasing access to PER2. During refeeding, decreased nuclear FOXO1 and suppression of AMPK activity would act in parallel to decrease *Abcg5/8* expression. Metformin treatment in the insulin resistant states might be expected to increase insulin action, decreasing nuclear FOXO1 and opposing the effects of increased AMPK activity. However, because metformin increased hepatic *Abcg5/8* expression in WTD-fed mice, the predominant effect of metformin is presumably exerted by the mechanisms described herein.

We show that activation of AMPK and inhibition of ACLY decrease Period 2 transcriptional inhibitory activity at the *Abcg5/8* locus. AMPK has been shown to decrease the stability of PER2 via an indirect pathway,⁴⁸ as well as PER2 binding partner CRY1 via phosphorylation-mediated degradation.³⁷ These findings link the negative limb of the circadian clock to *Abcg5/8* expression via PER2. The positive arm of the core circadian clock pathway involving BMAL1 has also been implicated in the regulation of *Abcg5/8* and cholesterol efflux. Pan et al⁶⁷ found that knockout of *Bmal1*, globally or in liver specifically, decreased *Abcg5/8* expression and consequently decreased cholesterol secretion into bile and feces and increased atherosclerosis. This regulation was indirect as BMAL1 regulated another transcription factor, *Gata4/6*, that directly bound to the *Abcg5/8* bicistronic promoter.

Metformin is a preferred initial treatment for type 2 diabetes mellitus in part because of an apparent benefit on atherosclerotic cardiovascular disease. The UKPDS Study (United Kingdom Prospective Diabetes Study) demonstrated that patients treated with metformin had a reduced risk of myocardial infarction, as well as decreased risk of diabetes mellitus-related deaths and all-cause mortality compared with a conventional therapy.¹ Moreover, patients with a history of coronary artery disease showed a significant decrease in cardiovascular events compared with patients given another class of anti-diabetic drug, glipizide.² Early studies with metformin showed a decrease in total cholesterol, LDL cholesterol, and triglyceride levels compared with control groups, in addition to increased HDL levels.^{3,68-71} However, more recent studies with a longer follow-up duration have not shown the same effects on lipoproteins.^{2,4} While human relevance is uncertain, our studies raise the possibility that the cardiovascular benefit of metformin could be explained in part by upregulation of *ABCG5/8*. Genetic ablation of *Abcg5/8* in mice resulted in decreased biliary cholesterol and increased VLDL cholesterol levels.⁹ Conversely, transgenic overexpression of human *ABCG5/8* in mice resulted in increased cholesterol excretion to bile, decreased VLDL/LDL cholesterol, and decreased atherosclerotic lesion size in LDLR-deficient mice, indicating an LDLR-independent mechanism of LDL reduction.⁸ Our findings provide partial support for the hypothesis that the beneficial effects of metformin may be explained by increased RCT. We tested the RCT hypothesis by injecting ³H-CE HDL into WTD-fed mice given daily injections of metformin. There was a significant increase in the initial rapid clearance of ³H-CE from plasma. However, there was only a trend for increased excretion of ³H-cholesterol in feces ($P=0.20$). This could be because

the 2 day fecal collection introduced too much variability to detect a transient initial effect. Alternatively, the increased *Ldlr* expression in liver could increase the uptake of nonradiolabeled LDL cholesterol, decreasing the specific activity of the hepatic and fecal ³H-cholesterol pool. The increased *Ldlr* mRNA may have arisen from increased expression of *ABCG5/8*, as well as inhibition of HMGCoA (3-hydroxy-3-methylglutaryl-CoA) reductase by AMPK activation.^{72,73} Together the findings suggest that both LDL cholesterol lowering and increased RCT could represent benefits that accrue from metformin, AMPK activation, and ACLY inhibition via upregulation of *ABCG5/8*.

Targeting ACLY has been suggested as a treatment for cancer,^{27,74,75} and recently inhibition of ACLY has proved to be beneficial in models of high fat, high cholesterol feeding.^{76,77} Targeted disruption of ACLY using adenoviral shRNA-mediated knockdown resulted in decreases in VLDL TG and decreased expression of genes involved in lipogenesis and TG synthesis.⁷⁶ In a hamster model on a high-fat high-cholesterol diet administration, an ACLY inhibitor, ETC-1002 (Bempedoic Acid⁷⁸), resulted in decreases in LDL and VLDL cholesterol along with decreases in hepatic CE and free cholesterol.⁷⁷ More recent studies with Bempedoic acid showed reduced atherosclerosis progression in an *Ldlr*^{-/-} mouse model, and significant increases in hepatic *Abcg5/8* mRNA expression were discovered by mRNA profiling.⁷⁹ Our studies provide a mechanism to explain the link between ACLY inhibition and increased hepatic *Abcg5/8* levels, involving the short-lived transcriptional repressor PER2. This could represent an important therapeutic benefit of this approach. Although increased biliary cholesterol secretion resulting from induction of *Abcg5/8* by metformin, or ACLY inhibition, might be expected to increase gallstone formation, we found that *Bsep* was upregulated by a similar mechanism to *Abcg5/8*, suggesting a coordinated mechanism to dispose of cholesterol without favoring gallstone formation. Our studies thus suggest several potential ways to link diabetes mellitus treatments with a beneficial effect on cardiovascular disease without increasing gallstone risk.

Sources of Funding

This study was supported by National Institutes of Health (NIH) grant HL107653 (A.R. Tall), and HL 87123 (A.R. Tall, D. Accili). M.M. Molusky was also supported by the T32 training grant from the NIH (HL007343) and J. Hsieh by the Gilead Sciences Liver Scholar Program. R.A. Haeusler and S.X. Lee were supported by HL125649.

Disclosures

None.

References

1. UK Prospective Diabetes Study (UKPDS) Group. Effect of intensive blood-glucose control with metformin on complications in overweight patients with type 2 diabetes (UKPDS 34). *Lancet*. 1998;352:854-865. doi: 10.1016/S0140-6736(98)07037-8.
2. Hong J, Zhang Y, Lai S, et al; SPREAD-DIMCAD Investigators. Effects of metformin versus glipizide on cardiovascular outcomes in patients with type 2 diabetes and coronary artery disease. *Diabetes Care*. 2013;36:1304-1311. doi: 10.2337/dc12-0719.
3. Jeppesen J, Zhou MY, Chen YD, Reaven GM. Effect of metformin on postprandial lipemia in patients with fairly to poorly controlled NIDDM. *Diabetes Care*. 1994;17:1093-1099.

4. Preiss D, Lloyd SM, Ford I, McMurray JJ, Holman RR, Welsh P, Fisher M, Packard CJ, Sattar N. Metformin for non-diabetic patients with coronary heart disease (the CAMERA study): a randomised controlled trial. *Lancet Diabetes Endocrinol*. 2014;2:116–124. doi: 10.1016/S2213-8587(13)70152-9.
5. Ferrannini E, DeFronzo RA. Impact of glucose-lowering drugs on cardiovascular disease in type 2 diabetes. *Eur Heart J*. 2015;36:2288–2296. doi: 10.1093/eurheartj/ehv239.
6. Fullerton MD, Ford RJ, McGregor CP, LeBlond ND, Snider SA, Stypa SA, Day EA, Lhoták Š, Schertzer JD, Austin RC, Kemp BE, Steinberg GR. Salicylate improves macrophage cholesterol homeostasis via activation of Ampk. *J Lipid Res*. 2015;56:1025–1033. doi: 10.1194/jlr.M058875.
7. Berge KE, Tian H, Graf GA, Yu L, Grishin NV, Schultz J, Kwiterovich P, Shan B, Barnes R, Hobbs HH. Accumulation of dietary cholesterol in sitosterolemia caused by mutations in adjacent ABC transporters. *Science*. 2000;290:1771–1775.
8. Yu L, Li-Hawkins J, Hammer RE, Berge KE, Horton JD, Cohen JC, Hobbs HH. Overexpression of ABCG5 and ABCG8 promotes biliary cholesterol secretion and reduces fractional absorption of dietary cholesterol. *J Clin Invest*. 2002;110:671–680. doi: 10.1172/JCI16001.
9. Yu L, Hammer RE, Li-Hawkins J, Von Bergmann K, Lutjohann D, Cohen JC, Hobbs HH. Disruption of Abcg5 and Abcg8 in mice reveals their crucial role in biliary cholesterol secretion. *Proc Natl Acad Sci USA*. 2002;99:16237–16242. doi: 10.1073/pnas.252582399.
10. Kathiresan S, Willer CJ, Peloso GM, et al. Common variants at 30 loci contribute to polygenic dyslipidemia. *Nat Genet*. 2009;41:56–65. doi: 10.1038/ng.291.
11. Teslovich TM, Musunuru K, Smith AV, et al. Biological, clinical and population relevance of 95 loci for blood lipids. *Nature*. 2010;466:707–713. doi: 10.1038/nature09270.
12. Teupser D, Baber R, Ceglarek U, et al. Genetic regulation of serum phyto-sterol levels and risk of coronary artery disease. *Circ Cardiovasc Genet*. 2010;3:331–339. doi: 10.1161/CIRCGENETICS.109.907873.
13. IBC 50K CAD Consortium. Large-scale gene-centric analysis identifies novel variants for coronary artery disease. *PLoS Genet*. 2011;7:e1002260. doi: 10.1371/journal.pgen.1002260.
14. Repa JJ, Berge KE, Pomajzl C, Richardson JA, Hobbs H, Mangelsdorf DJ. Regulation of ATP-binding cassette sterol transporters ABCG5 and ABCG8 by the liver X receptors alpha and beta. *J Biol Chem*. 2002;277:18793–18800. doi: 10.1074/jbc.M109927200.
15. van der Veen JN, Havinga R, Bloks VW, Groen AK, Kuipers F. Cholesterol feeding strongly reduces hepatic VLDL-triglyceride production in mice lacking the liver X receptor alpha. *J Lipid Res*. 2007;48:337–347. doi: 10.1194/jlr.M600170-JLR200.
16. Biddinger SB, Haas JT, Yu BB, Bezy O, Jing E, Zhang W, Unterman TG, Carey MC, Kahn CR. Hepatic insulin resistance directly promotes formation of cholesterol gallstones. *Nat Med*. 2008;14:778–782. doi: 10.1038/nm1785.
17. Haeussler RA, Pratt-Hyatt M, Welch CL, Klaassen CD, Accili D. Impaired generation of 12-hydroxylated bile acids links hepatic insulin signaling with dyslipidemia. *Cell Metab*. 2012;15:65–74. doi: 10.1016/j.cmet.2011.11.010.
18. Bailey CJ, Matty AJ. Glucose tolerance and plasma insulin of the rat in relation to the oestrous cycle and sex hormones. *Horm Metab Res*. 1972;4:266–270. doi: 10.1055/s-0028-1094063.
19. Paigen B, Morrow A, Brandon C, Mitchell D, Holmes P. Variation in susceptibility to atherosclerosis among inbred strains of mice. *Atherosclerosis*. 1985;57:65–73.
20. Postic C, Shiota M, Niswender KD, Jetton TL, Chen Y, Moates JM, Shelton KD, Lindner J, Cherrington AD, Magnuson MA. Dual roles for glucokinase in glucose homeostasis as determined by liver and pancreatic beta cell-specific gene knock-outs using Cre recombinase. *J Biol Chem*. 1999;274:305–315.
21. Nakada D, Saunders TL, Morrison SJ. Lkb1 regulates cell cycle and energy metabolism in haematopoietic stem cells. *Nature*. 2010;468:653–658. doi: 10.1038/nature09571.
22. Lagor WR, Brown RJ, Toh SA, Millar JS, Fuki IV, de la Llera-Moya M, Yuen T, Rothblat G, Billheimer JT, Rader DJ. Overexpression of apolipoprotein F reduces HDL cholesterol levels in vivo. *Arterioscler Thromb Vasc Biol*. 2009;29:40–46. doi: 10.1161/ATVBAHA.108.177105.
23. Föger B, Santamarina-Fojo S, Shamburek RD, Parrot CL, Talley GD, Brewer HB Jr. Plasma phospholipid transfer protein. Adenovirus-mediated overexpression in mice leads to decreased plasma high density lipoprotein (HDL) and enhanced hepatic uptake of phospholipids and cholesteryl esters from HDL. *J Biol Chem*. 1997;272:27393–27400.
24. Tollefson JH, Albers JJ. Isolation, characterization, and assay of plasma lipid transfer proteins. *Methods Enzymol*. 1986;129:797–816.
25. Folch J, Lees M, Sloane Stanley GH. A simple method for the isolation and purification of total lipides from animal tissues. *J Biol Chem*. 1957;226:497–509.
26. Ye R, Selby CP, Ozturk N, Annayev Y, Sancar A. Biochemical analysis of the canonical model for the mammalian circadian clock. *J Biol Chem*. 2011;286:25891–25902. doi: 10.1074/jbc.M111.254680.
27. Wellen KE, Hatzivassiliou G, Sachdeva UM, Bui TV, Cross JR, Thompson CB. ATP-citrate lyase links cellular metabolism to histone acetylation. *Science*. 2009;324:1076–1080. doi: 10.1126/science.1164097.
28. Lee JV, Carrer A, Shah S, et al. Akt-dependent metabolic reprogramming regulates tumor cell histone acetylation. *Cell Metab*. 2014;20:306–319. doi: 10.1016/j.cmet.2014.06.004.
29. Madiraju AK, Erion DM, Rahimi Y, et al. Metformin suppresses gluco-neogenesis by inhibiting mitochondrial glycerophosphate dehydrogenase. *Nature*. 2014;510:542–546. doi: 10.1038/nature13270.
30. Cool B, Zinker B, Chiou W, et al. Identification and characterization of a small molecule AMPK activator that treats key components of type 2 diabetes and the metabolic syndrome. *Cell Metab*. 2006;3:403–416. doi: 10.1016/j.cmet.2006.05.005.
31. Hardie DG. The AMP-activated protein kinase pathway—new players upstream and downstream. *J Cell Sci*. 2004;117(pt 23):5479–5487. doi: 10.1242/jcs.01540.
32. Assifi MM, Suchankova G, Constant S, Prentki M, Saha AK, Ruderman NB. AMP-activated protein kinase and coordination of hepatic fatty acid metabolism of starved/carbohydrate-refed rats. *Am J Physiol Endocrinol Metab*. 2005;289:E794–E800. doi: 10.1152/ajpendo.00144.2005.
33. Dentin R, Benhamed F, Pégories JP, Foufelle F, Viollet B, Vaulont S, Girard J, Postic C. Polyunsaturated fatty acids suppress glycolytic and lipogenic genes through the inhibition of ChREBP nuclear protein translocation. *J Clin Invest*. 2005;115:2843–2854. doi: 10.1172/JCI25256.
34. Yamauchi T, Kamon J, Minokoshi Y, et al. Adiponectin stimulates glucose utilization and fatty-acid oxidation by activating AMP-activated protein kinase. *Nat Med*. 2002;8:1288–1295. doi: 10.1038/nm788.
35. Woo SL, Xu H, Li H, et al. Metformin ameliorates hepatic steatosis and inflammation without altering adipose phenotype in diet-induced obesity. *PLoS One*. 2014;9:e91111. doi: 10.1371/journal.pone.0091111.
36. Lindholm CR, Ertel RL, Bauwens JD, Schmuck EG, Mulligan JD, Saue KW. A high-fat diet decreases AMPK activity in multiple tissues in the absence of hyperglycemia or systemic inflammation in rats. *J Physiol Biochem*. 2013;69:165–175. doi: 10.1007/s13105-012-0199-2.
37. Lamia KA, Sachdeva UM, DiTacchio L, Williams EC, Alvarez JG, Egan DF, Vasquez DS, Juguilon H, Panda S, Shaw RJ, Thompson CB, Evans RM. AMPK regulates the circadian clock by cryptochrome phosphorylation and degradation. *Science*. 2009;326:437–440. doi: 10.1126/science.1172156.
38. Esquejo RM, Salatto CT, Delmore J, et al. Activation of liver AMPK with PF-06409577 corrects NAFLD and lowers cholesterol in rodent and primate preclinical models. *EBioMedicine*. 2018;31:122–132. doi: 10.1016/j.ebiom.2018.04.009.
39. Peet DJ, Turely SD, Ma W, Janowski BA, Lobaccaro JM, Hammer RE, Mangelsdorf DJ. Cholesterol and bile acid metabolism are impaired in mice lacking the nuclear oxysterol receptor LXR alpha. *Cell*. 1998;93:693–704.
40. Repa JJ, Mangelsdorf DJ. Nuclear receptor regulation of cholesterol and bile acid metabolism. *Curr Opin Biotechnol*. 1999;10:557–563.
41. Apfel R, Benbrook D, Lernhardt E, Ortiz MA, Salbert G, Pfahl M. A novel orphan receptor specific for a subset of thyroid hormone-responsive elements and its interaction with the retinoid/thyroid hormone receptor subfamily. *Mol Cell Biol*. 1994;14:7025–7035.
42. Sobell HM. Actinomycin and DNA transcription. *Proc Natl Acad Sci USA*. 1985;82:5328–5331.
43. Hughes ME, DiTacchio L, Hayes KR, Vollmers C, Pulivarthy S, Baggs JE, Panda S, Hogenesch JB. Harmonics of circadian gene transcription in mammals. *PLoS Genet*. 2009;5:e1000442. doi: 10.1371/journal.pgen.1000442.
44. Koike N, Yoo SH, Huang HC, Kumar V, Lee C, Kim TK, Takahashi JS. Transcriptional architecture and chromatin landscape of the core circadian clock in mammals. *Science*. 2012;338:349–354. doi: 10.1126/science.1226339.
45. Panda S, Antoch MP, Miller BH, Su AI, Schook AB, Straume M, Schultz PG, Kay SA, Takahashi JS, Hogenesch JB. Coordinated transcription of key pathways in the mouse by the circadian clock. *Cell*. 2002;109:307–320.
46. Jin X, Shearman LP, Weaver DR, Zylka MJ, de Vries GJ, Reppert SM. A molecular mechanism regulating rhythmic output from the suprachiasmatic circadian clock. *Cell*. 1999;96:57–68.

47. Duong HA, Robles MS, Knutti D, Weitz CJ. A molecular mechanism for circadian clock negative feedback. *Science*. 2011;332:1436–1439. doi: 10.1126/science.1196766.
48. Um JH, Yang S, Yamazaki S, Kang H, Viollet B, Foretz M, Chung JH. Activation of 5'-AMP-activated kinase with diabetes drug metformin induces casein kinase Iε (CKIε)-dependent degradation of clock protein mPer2. *J Biol Chem*. 2007;282:20794–20798. doi: 10.1074/jbc.C700070200.
49. Nishii K, Yamanaka I, Yasuda M, Kiyohara YB, Kitayama Y, Kondo T, Yagita K. Rhythmic post-transcriptional regulation of the circadian clock protein mPER2 in mammalian cells: a real-time analysis. *Neurosci Lett*. 2006;401:44–48. doi: 10.1016/j.neulet.2006.03.022.
50. Field MD, Maywood ES, O'Brien JA, Weaver DR, Reppert SM, Hastings MH. Analysis of clock proteins in mouse SCN demonstrates phylogenetic divergence of the circadian clockwork and resetting mechanisms. *Neuron*. 2000;25:437–447.
51. Asher G, Gatfield D, Stratmann M, Reinke H, Dibner C, Kreppel F, Mostoslavsky R, Alt FW, Schibler U. SIRT1 regulates circadian clock gene expression through PER2 deacetylation. *Cell*. 2008;134:317–328. doi: 10.1016/j.cell.2008.06.050.
52. Watson JA, Fang M, Lowenstein JM. Tricarballoylate and hydroxycitrate: substrate and inhibitor of ATP: citrate oxaloacetate lyase. *Arch Biochem Biophys*. 1969;135:209–217.
53. Linn TC, Srere PA. Binding of ATP citrate lyase to the microsomal fraction of rat liver. *J Biol Chem*. 1984;259:13379–13384.
54. Damiola F, Le Minh N, Preitner N, Kormann B, Fleury-Olela F, Schibler U. Restricted feeding uncouples circadian oscillators in peripheral tissues from the central pacemaker in the suprachiasmatic nucleus. *Genes Dev*. 2000;14:2950–2961.
55. Ma Z, Chu CH, Cheng D. A novel direct homogeneous assay for ATP citrate lyase. *J Lipid Res*. 2009;50:2131–2135. doi: 10.1194/jlr.D900008-JLR200.
56. Li JJ, Wang H, Tino JA, et al. 2-hydroxy-N-arylbzenesulfonamides as ATP-citrate lyase inhibitors. *Bioorg Med Chem Lett*. 2007;17:3208–3211. doi: 10.1016/j.bmcl.2007.03.017.
57. Gatfield D, Schibler U. Physiology. Proteasomes keep the circadian clock ticking. *Science*. 2007;316:1135–1136. doi: 10.1126/science.1144165.
58. Hirano A, Yumimoto K, Tsunematsu R, Matsumoto M, Oyama M, Kozuka-Hata H, Nakagawa T, Lanjakornsiripan D, Nakayama KI, Fukada Y. FBXL21 regulates oscillation of the circadian clock through ubiquitination and stabilization of cryptochromes. *Cell*. 2013;152:1106–1118. doi: 10.1016/j.cell.2013.01.054.
59. Yoo SH, Mohawk JA, Slepka SM, et al. Competing E3 ubiquitin ligases govern circadian periodicity by degradation of CRY in nucleus and cytoplasm. *Cell*. 2013;152:1091–1105. doi: 10.1016/j.cell.2013.01.055.
60. Schmalen I, Reischl S, Wallach T, Klemz R, Grudziecki A, Prabu JR, Benda C, Kramer A, Wolf E. Interaction of circadian clock proteins CRY1 and PER2 is modulated by zinc binding and disulfide bond formation. *Cell*. 2014;157:1203–1215. doi: 10.1016/j.cell.2014.03.057.
61. Ho KJ, Drummond JL. Circadian rhythm of biliary excretion and its control mechanisms in rats with chronic biliary drainage. *Am J Physiol*. 1975;229:1427–1437. doi: 10.1152/ajplegacy.1975.229.5.1427.
62. Metzger AL, Adler R, Heysfield S, Grundy SM. Diurnal variation in biliary lipid composition. Possible role in cholesterol gallstone formation. *N Engl J Med*. 1973;288:333–336. doi: 10.1056/NEJM197302152880702.
63. Northfield TC, Hofmann AF. Biliary lipid secretion in gallstone patients. *Lancet*. 1973;1:747–748.
64. Bloch HM, Thornton JR, Heaton KW. Effects of fasting on the composition of gallbladder bile. *Gut*. 1980;21:1087–1089.
65. Shaffer EA, Braasch JW, Small DM. Bile composition at and after surgery in normal persons and patients with gallstones. Influence of cholecystectomy. *N Engl J Med*. 1972;287:1317–1322. doi: 10.1056/NEJM197212282872603.
66. Carling D, Zammit VA, Hardie DG. A common bicyclic protein kinase cascade inactivates the regulatory enzymes of fatty acid and cholesterol biosynthesis. *FEBS Lett*. 1987;223:217–222.
67. Pan X, Bradfield CA, Hussain MM. Global and hepatocyte-specific ablation of Bmal1 induces hyperlipidaemia and enhances atherosclerosis. *Nat Commun*. 2016;7:13011. doi: 10.1038/ncomms13011.
68. Giugliano D, De Rosa N, Di Maro G, Marfella R, Acampora R, Buoninconti R, D'Onofrio F. Metformin improves glucose, lipid metabolism, and reduces blood pressure in hypertensive, obese women. *Diabetes Care*. 1993;16:1387–1390.
69. Hollenbeck CB, Johnston P, Varasteh BB, Chen YD, Reaven GM. Effects of metformin on glucose, insulin and lipid metabolism in patients with mild hypertriglyceridaemia and non-insulin dependent diabetes by glucose tolerance test criteria. *Diabetes Metab*. 1991;17:483–489.
70. Reaven GM, Johnston P, Hollenbeck CB, Skowronski R, Zhang JC, Goldfine ID, Chen YD. Combined metformin-sulfonylurea treatment of patients with noninsulin-dependent diabetes in fair to poor glycaemic control. *J Clin Endocrinol Metab*. 1992;74:1020–1026. doi: 10.1210/jcem.74.5.1569149.
71. Robinson AC, Burke J, Robinson S, Johnston DG, Elkeles RS. The effects of metformin on glycaemic control and serum lipids in insulin-treated NIDDM patients with suboptimal metabolic control. *Diabetes Care*. 1998;21:701–705.
72. Beg ZH, Allmann DW, Gibson DM. Modulation of 3-hydroxy-3-methylglutaryl coenzyme A reductase activity with cAMP and with protein fractions of rat liver cytosol. *Biochem Biophys Res Commun*. 1973;54:1362–1369.
73. Henin N, Vincent MF, Gruber HE, Van den Berghe G. Inhibition of fatty acid and cholesterol synthesis by stimulation of AMP-activated protein kinase. *FASEB J*. 1995;9:541–546.
74. Bauer DE, Hatzivassiliou G, Zhao F, Andreadis C, Thompson CB. ATP citrate lyase is an important component of cell growth and transformation. *Oncogene*. 2005;24:6314–6322. doi: 10.1038/sj.onc.1208773.
75. Hatzivassiliou G, Zhao F, Bauer DE, Andreadis C, Shaw AN, Dhanak D, Hingorani SR, Tuveson DA, Thompson CB. ATP citrate lyase inhibition can suppress tumor cell growth. *Cancer Cell*. 2005;8:311–321. doi: 10.1016/j.ccr.2005.09.008.
76. Wang Q, Li S, Jiang L, Zhou Y, Li Z, Shao M, Li W, Liu Y. Deficiency in hepatic ATP-citrate lyase affects VLDL-triglyceride mobilization and liver fatty acid composition in mice. *J Lipid Res*. 2010;51:2516–2526. doi: 10.1194/jlr.M003335.
77. Pinkosky SL, Filippov S, Srivastava RA, Hanselman JC, Bradshaw CD, Hurley TR, Cramer CT, Spahr MA, Brant AF, Houghton JL, Baker C, Naples M, Adeli K, Newton RS. AMP-activated protein kinase and ATP-citrate lyase are two distinct molecular targets for ETC-1002, a novel small molecule regulator of lipid and carbohydrate metabolism. *J Lipid Res*. 2013;54:134–151. doi: 10.1194/jlr.M030528.
78. Pinkosky SL, Newton RS, Day EA, Ford RJ, Lhotak S, Austin RC, Birch CM, Smith BK, Filippov S, Groot PH, Steinberg GR, Lalwani ND. Liver-specific ATP-citrate lyase inhibition by bempedoic acid decreases LDL-C and attenuates atherosclerosis. *Nat Commun*. 2016;7:13457. doi: 10.1038/ncomms13457.
79. Samsouondar JP, Burke AC, Sutherland BG, Telford DE, Sawyez CG, Edwards JY, Pinkosky SL, Newton RS, Huff MW. Prevention of diet-induced metabolic dysregulation, inflammation, and atherosclerosis in Ldlr^{-/-} mice by treatment with the ATP-citrate lyase inhibitor bempedoic acid. *Arterioscler Thromb Vasc Biol*. 2017;37:647–656. doi: 10.1161/ATVBAHA.116.308963.

Highlights

- Metformin induces expression of the sterol transporters *Abcg5/8* (ATP-binding cassette transporter G5/G8) by decreasing Period 2 occupancy on the *Abcg5/8* promoter.
- Our mechanistic data suggests a link between cholesterol excretion and hepatic lipogenic activity and circadian rhythm.
- The findings suggest that both LDL (low-density lipoprotein) cholesterol lowering and increased reverse cholesterol transport could represent benefits that accrue from metformin, AMPK (5' adenosine monophosphate-activated protein kinase) activation and ACLY inhibition via upregulation of *ABCG5/8*.